

# Numerical study of thermal conductivity effects on stability of the reversed-field pinch.

Ahmed Akram Mirza, Jan Scheffel

*Division of Fusion Plasma Physics, Association EURATOM – VR, Alfvén Laboratory,*

*School of Electrical Engineering, Royal Institute of Technology,*

*SE - 10044 Stockholm, Sweden*

## 1. Introduction

Tearing modes presently dominate fluctuations in the reversed-field pinch (RFP). Using current profile control techniques, tearing modes can be removed, and resistive pressure driven modes become more significant. The plasma confinement properties in the RFP are considerably limited by the resistive “g-modes”. In the tokamak, however, these resistive g-modes can be eliminated due to stabilizing curvature effects. In the RFP, classical theory predicts that resistive g-modes are linearly unstable for all equilibria. These instabilities may cause modest global energy confinement parameters, preventing the RFP from operating at high poloidal beta values, being crucial for a commercial fusion reactor. In earlier work, Bruno et.al [1] have proposed the stabilization of resistive g-modes in the RFP by including finite perpendicular thermal diffusion effects. In this work, we present a computational analysis of stability of resistive pressure driven modes with and without heat conductivity effects.

## 2. Calculation of growth rate by $\Delta'$ analysis

First approach is to solve the linear stability by means of asymptotic matching, known in literature as  $\Delta'$  analysis [2]. The plasma has very small resistivity, the contribution of which is considered in a very thin layer, so-called resistive layer. Both types of energy equations, without and with heat conduction terms, are studied. In particular, we determine to what extent the orderings used in the  $\Delta'$  theory limit its validity.

### 2.1 $\Delta'$ Stability analysis with adiabatic energy equation

As stated earlier, resistive MHD modes have early been investigated by using the traditional dispersion relation [1]

$$r_s \Delta' = 2\pi \frac{\Gamma(\frac{3}{4})}{\Gamma(\frac{1}{4})} Q^{\frac{5}{4}} \left( 1 - \frac{\pi D}{4Q^{\frac{3}{2}}} \right) \quad (1)$$

where  $r_s$  is the radial location of resonance,  $\Delta'$  is defined as the jump across the resonance of the logarithmic derivative of the radial component of perturbed magnetic field,  $D$  is Suydam's normalized pressure gradient and  $Q$  is the normalized growth rate. In order to calculate the growth rates, a numerical shooting procedure has been employed. The code is designed in

such a way that, at low poloidal beta values, it permits benchmarking with zero-pressure  $\Delta'$  theory [2].

## 2.2. $\Delta'$ Stability analysis including thermal conductivity

In a recent  $\Delta'$  analysis, using a new tearing mode ordering for the resistive layer dynamics, it is claimed, however, that the traditional adiabatic assumption for the energy equation is not justified [1]. Instead, inclusion of thermal conductivity allegedly flattens the pressure profile near the resistive layer and stabilizes resistive MHD modes at moderate plasma beta. An extended energy equation has been used with the assumption of constant density. The dispersion relation obtained from this model is [1]

$$r_s \Delta' = 2\pi \frac{\Gamma(\frac{3}{4})}{\Gamma(\frac{1}{4})} Q^{\frac{5}{4}} - \frac{\pi^{\frac{3}{2}} r_s D}{2 \delta_x} \quad (2)$$

where

$$\delta_x = \left[ \frac{\chi_{\perp}}{\chi_{\parallel}} \frac{B^2}{m^2 B_{\theta}^2} \left( \left( \frac{r_s q_s}{q_s'} \right)^2 \right)^{\frac{1}{4}} \right] \quad (3)$$

Here,  $\delta_x$  is the new scale resonant layer length,  $m$  is the poloidal mode number,  $\chi_{\perp}$  and  $\chi_{\parallel}$  are the perpendicular and parallel thermal diffusivities respectively.

## 3. Time spectral weighted residual method

The second procedure is to solve the full set of resistive MHD equations in the entire spatial region. The results obtained from the  $\Delta'$  analysis are thus compared with an initial-value code that uses a fully resistive, linearised model for the entire plasma domain. The code is based on the novel generalized weighted residual method (GWRM), which is a fully spectral method for initial value problems in the form of partial differential equations [4]. The trial basis functions used for all temporal, spatial and physical domains are Chebyshev polynomials owing to their minimax property, which provides fast convergence [3]. A brief overview of GWRM follows. Consider the following first order parabolic or hyperbolic partial differential

equation.

$$\frac{\partial \mathbf{u}}{\partial t} = \mathbf{D}\mathbf{u} + \mathbf{f} \quad (4)$$

where  $\mathbf{u} = \mathbf{u}(t, \mathbf{x}; p)$  is the solution vector,  $\mathbf{D}$  is the linear or nonlinear matrix operator and  $\mathbf{f} = \mathbf{f}(t, \mathbf{x}; p)$  is a source term. Integrating equation (4) gives

$$\mathbf{u}(t, \mathbf{x}; p) = \mathbf{u}(t_0, \mathbf{x}; p) + \int_{t_0}^t \{ \mathbf{D}\mathbf{u}(t', \mathbf{x}; p) + \mathbf{f}(t', \mathbf{x}; p) \} dt' \quad (5)$$

where  $\mathbf{u}(t_0, \mathbf{x}; p)$  is chosen to satisfy the boundary as well as initial condition. Now, the starting point is approximating the solution vector with 1<sup>st</sup> kind, finite, multivariate Chebyshev polynomial series as both trial and weight functions. Confining here to a single dimensional domain, the solution ansatz can be written as the sum

$$u(t, x; p) = \sum_{k=0}^K \sum_{l=0}^L \sum_{m=0}^M a'_{klm} T_k(\tau) T_l(\xi) T_m(P) \quad (6)$$

with  $\tau, \xi, P$  being (shifted) time, space, and parameter free variables.

Prime denotes division of constant coefficient term by 2. As in traditional weighted residual methods (WRM), the unknown coefficients ' $a'_{klm}$ ' are determined by requiring that the integral of the weighted residual, obtained from (5) and (6), over the computational domain is zero. Performing the integration by parts, the details of which can be found in [4], this results

$$a_{qrs} = 2\delta_{q0}b_{rs} + A_{qrs} + F_{qrs} \quad (7)$$

This GWRM coefficient equation is a complete implicit relation together with the boundary conditions. ' $A_{qrs}$ ' are functions of coefficients ' $a_{qrs}$ ', result from the operator  $D$ , the coefficients ' $b_{rs}$ ' reflect the initial conditions while ' $F_{qrs}$ ' are uniquely determined from the source term ' $f$ '. Equation (7) can be linear or nonlinear depending upon the type of the problem. If linear, coefficients can be found using traditional methods like Gauss elimination method. In case of nonlinear equation (7), a semi implicit root solver SIR [4] has been designed which has shown excellent compatibility for GWRM.

#### 4. Results

For numerical comparison, the following RFP equilibrium profiles (given in [2]) are used with  $\beta_\theta = 0.046$  for both  $\Delta'$  and GWRM. Here  $m=1$ ,  $k_z=2$  (axial mode number) and all quantities are normalized [1].

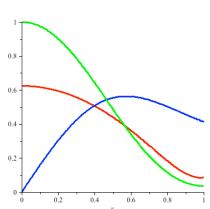


Fig.1 RFP Equilibrium profiles

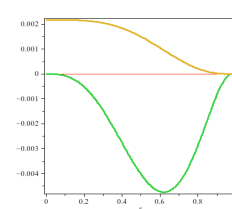


Fig.2 RFP eq. Pressure profiles

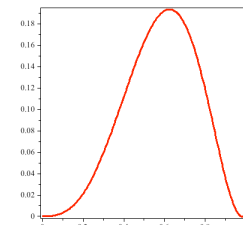


Fig.3 Suydam's criterion profile.

#### 4.1 Growth rate by $\Delta'$ analysis

In the figures below, we have shown growth rate dependence on resistivity for  $\beta_\theta = 0.046$ . It can be seen that growth rate increases, when heat conduction terms are included for this specific equilibrium.

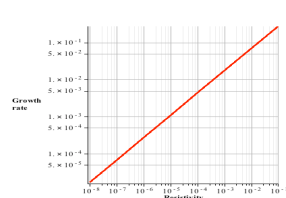


Fig.4 Growth rate by  $\Delta'$  (without heat conductivity)

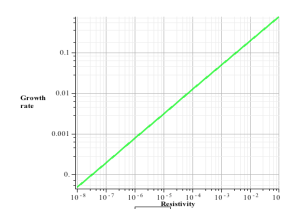


Fig.5 Growth rate by  $\Delta'$  (with heat conductivity)

## 4.2 Growth rates by GWRM

GWRM gives the complete solution and thus plays a vital role for calculations of growth rate, which are in good agreement with those values obtained by  $\Delta'$ .

### 4.2.1. Without heat conductivity

Figures 6 and 7 show the growth rate of perturbed radial velocity and magnetic field. For Lundquist number  $S_0 = 10^{-3}$ , growth rate = 0.011. Figures (8&9) show the time evolution of the growth rate of radial velocity and magnetic field.

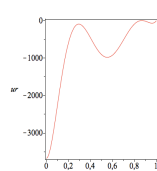


Fig.6 Perturbed radial velocity

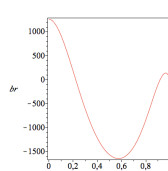


Fig.7 Perturbed radial magnetic field

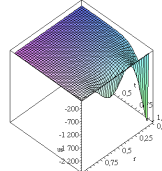


Fig.8 Perturbed radial vel.

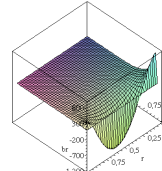


Fig.9 Perturbed magnetic field

### 4.2.2. With heat conductivity

For evaluation of heat conduction terms, plasma parameters from EXTRAP T2R (Sweden) have been used. For this specific equilibrium, we obtained  $\chi_{\perp} = 2.54 \cdot 10^{-7}$ ,  $\chi_{\parallel} = 0.68 \cdot 10^{-5}$ . For  $S_0 = 10^{-3}$ , growth rate = 0.048 which implies that the resistive g-modes turn out to be more unstable. The figures (10&11) show growth rate of radial velocity and magnetic field. Figures (12&13) show the time evolution of the growth rate of radial velocity and magnetic field.

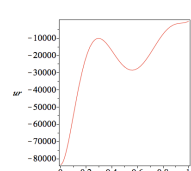


Fig.10. Perturbed magnetic field

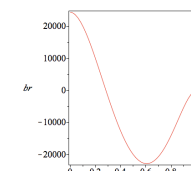


Fig.11. Perturbed radial vel.

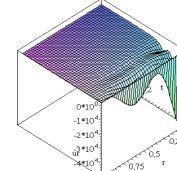


Fig.12 3D Pert. radial vel.

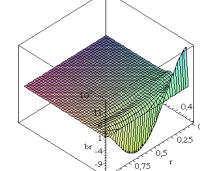


Fig.13. 3D Pert. mag. field

## 5. Conclusion

The preliminary numerical study by both  $\Delta'$  and GWRM does not support the claim that, inclusion of heat conductivity in the energy equation, somehow provides marginal stability and stabilizes the pressure driven modes in the RFP.

## 6. References

- [1] A. Bruno et.al, *Physics of plasmas*, volume 10 (2005), number 6
- [2] Jin Li et.al , *Computational studies of MHD stability for RFP and tokamaks*, TRITA-EE 1999:356, Royal Institute of Technology, Stockholm, Sweden (1999).
- [3] Mason, J. C., & Handscomb, D. C., *Chebyshev Polynomials*, Chapman and Hall/CRC, (2003)
- [4] J. Scheffel, *Time-Spectral Solution of Initial-Value Problems*, Ch 1 in *Partial Differential Equations: Theory, Analysis and Applications*, Nova Science Publishers, Inc. 2011